CrystEngComm

RSC Publishing

COMMUNICATION

View Article Online
View Journal | View Issue

Ionic liquid-assisted solvothermal synthesis of oriented self-assembled Fe_3O_4 nanoparticles into monodisperse nanoflakes†

Cite this: *CrystEngComm*, 2013, **15**, 3284

Received 8th January 2013,
Accepted 25th February 2013

DOI: 10.1039/c3ce00035d

www.rsc.org/crystengcomm

Xiaodi Liu,[ab] Xiaochuan Duan,[a] Qing Qin,[a] Qinglun Wang[c] and Wenjun Zheng*[a]

Self-assembled Fe_3O_4 nanoflakes have been synthesized *via* an ionic liquid-assisted solvothermal method. The obtained Fe_3O_4 nanoflakes are composed of well-aligned nanoparticles with an average diameter of about 15 nm. More importantly, the ionic liquid [C_{16}mim]Cl (1-hexadecyl-3-methylimidazolium chloride) plays a critical role for the self-assembly of nanoparticles into nanoflakes by adsorbing onto the surfaces of the primary Fe_3O_4 nanoparticles.

Recently, many research efforts in nanoscience have been devoted to the self-assembly of nanoscale building blocks into well-defined 2D/3D superstructures, which could prevent the agglomeration of nanomaterials and supply more tunable and unique properties.[1] Nanoscale Fe_3O_4, as a type of conventional magnetic material, has been used in many fields owing to its unique electric and magnetic properties.[2] However, it was found that the "superparamagnetic limit", namely conflict between reducing the magnetic energy barrier and decreasing the size, restrains the development of Fe_3O_4 nanomaterials.[3] To some extent, Fe_3O_4 superstructures could overcome this limit and some researchers have concentrated on the synthesis of self-assembled Fe_3O_4 superstructures.[4] Nevertheless, there are only a few reports on the synthesis of Fe_3O_4 superstructures self-assembled from nanoparticles.[5,6] In this regard, it is a challenge to explore novel routes for preparing nanoparticle-assembled Fe_3O_4 superstructures with good monodispersity and special magnetic properties.

Ionic liquids (ILs), consisting of organic cations and inorganic anions, have been wildly used in the inorganic nanomaterials community. ILs derived from 1-alkyl-3-methylimidazolium are of particular interest for their many favorable physico-chemical properties and wide synthetic applications.[7] Therein, long-chain ILs possess both lyotropic and thermotropic liquid-crystal properties and tend to self-assemble into ordered structures. Thus, they have been used as templates in the synthesis of nanomaterials.[8,9] Nevertheless, to the best of our knowledge, the exploration of their potential applications in the synthesis of self-assembled nanomaterials has been scarcely reported. In this paper, we present a novel and effective IL-assisted solvothermal method for the synthesis of nanoparticle-assembled Fe_3O_4 nanoflakes using [C_{16}mim]Cl (1-hexadecyl-3-methylimidazolium chloride) as a template. Moreover, it is found that the morphology of the product exerts a remarkable effect on its magnetic property.

The Fe_3O_4 nanoflakes were synthesized in 7.5 ml of distilled water–glycerol (the volume ratio is 1 : 2) together with 0.03 g of $FeCl_2{\cdot}4H_2O$, 0.40 g of [C_{16}mim]Cl and 2.5 ml of $N_2H_4{\cdot}H_2O$ at 180 °C for 24 h. The structure and morphology of the as-prepared Fe_3O_4 nanoflakes were studied by TEM, HRTEM, XRD and SEM. As displayed in Fig. 1a, one can clearly see that the products with an average diameter of 500 nm have good monodispersity and are composed of nanoparticles, which is in good agreement with the results observed in the SEM images (Fig. S1, ESI†). An HRTEM image taken at the fringe of a typical nanoflake (Fig. 1b) reveals that the original Fe_3O_4 nanoparticles have a mean size of about 15 nm. The clear lattice image shows that these nanoparticles are well-crystallized crystals with a *d*-spacing of 0.252 nm, corresponding to the lattice spacing of the (311) plane in cubic Fe_3O_4. This feature proves that the Fe_3O_4 nanoflakes are stacked by edge-by-edge "oriented attachment" of the nanoparticles.[10] In addition, the corresponding FFT pattern (inset of Fig. 1b) shows that the primary Fe_3O_4 nanoparticles are single crystals. The TEM image of some Fe_3O_4 nanoflakes standing perpendicular to the copper mesh (Fig. 1c) shows that the average thickness of the nanoflakes (~15 nm) is close to the diameter of the original nanoparticle, which can further substantiate the "oriented attachment" mechanism.[11] Furthermore, an HRTEM image (inset of Fig. 1c) shows a lattice spacing of 0.252 nm, which is also consistent with the (311) *d*-spacing of cubic Fe_3O_4. Fig. 1d depicts the XRD pattern of the Fe_3O_4 nanoflakes. The position and relative intensity of all

[a]*Department of Materials Chemistry, Key Laboratory of Advanced Energy Materials Chemistry (MOE) and TKL of Metal and Molecule-Based Material Chemistry, College of Chemistry, Nankai University, Tianjin, P. R. China. E-mail: zhwj@nankai.edu.cn*
[b]*College of Chemistry and Pharmaceutical Engineering, Nanyang Normal University, Nanyang, Henan, P. R. China*
[c]*Department of Chemistry, College of Chemistry, Nankai University, Tianjin, P. R. China*

† Electronic supplementary information (ESI) available: SEM images and XPS spectra of the Fe_3O_4 nanoflakes; crystal structure of the cubic Fe_3O_4; SEM and TEM images of the products obtained from the control experiments. See DOI: 10.1039/c3ce00035d

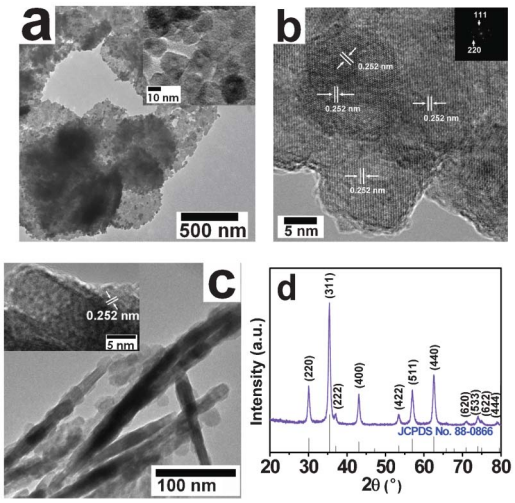

Fig. 1 (a) TEM image of the Fe_3O_4 nanoflakes. The inset is the higher-magnification TEM image of a typical nanoflake; (b) HRTEM image of a Fe_3O_4 nanoflake lying flat on the substrate and the inset is the FFT pattern of the primary nanoparticle; (c) TEM image of several Fe_3O_4 nanoflakes standing perpendicular to the substrate and the inset is the HRTEM image; (d) XRD pattern of the Fe_3O_4 nanoflakes.

the diffraction peaks match well with the standard XRD pattern of Fe_3O_4 (JCPDS No. 88-0866). Based on the Scherrer' formula, the average crystallite size of Fe_3O_4 is calculated to be *ca.* 15.4 nm by using the FWHM intensity of the (311) peak of Fe_3O_4.

Fe_3O_4 has an inverse spinel structure similar to that of γ-Fe_2O_3[12] so we therefore used XPS to distinguish the two phases and the survey spectrum is shown in Fig. S2, ESI.† In the XPS spectrum of Fe 2p (inset of Fig. 2a), two peaks (FWHM given in parentheses) at 724.7 (3.1) and 710.6 (2.9) eV are assigned to Fe $2p_{1/2}$ and Fe $2p_{3/2}$, respectively. Moreover, no satellite peak at ~719.0 eV is identified, clearly excluding the γ-Fe_2O_3 form.[13] A multiplet is found to be useful for the fitting of the Fe $2p_{3/2}$ spectrum for Fe_3O_4 and the Fe $2p_{3/2}$ spectrum is displayed in Fig. 2a. It can be seen that the Fe^{3+} multiplet peaks (1, 2, 3, and 4) and Fe^{2+} multiplet peaks (5, 6, and 7) are overlapped. Similar to the literature,[14] the intensity found for the Fe^{3+} and Fe^{2+} multiplets reveals that they are high spin and the Fe^{3+} : Fe^{2+} ratio is calculated to be about 1.7 : 1, which is close to that of 2 : 1 for

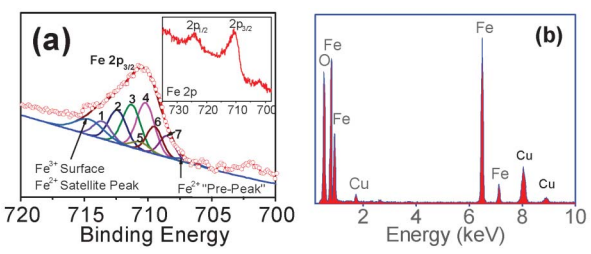

Fig. 2 (a) Fe $2p_{3/2}$ spectrum of the Fe_3O_4. The inset is the high-resolution XPS spectrum of Fe 2p, Fe^{3+} multiplet peaks: 1–4, Fe^{2+} multiplet peaks: 5–7; (b) EDS analysis for the Fe_3O_4, in which the Cu peaks are generated from the supporting copper meshes.

Fe_3O_4. The Fe/O ratio of Fe_3O_4 nanoflakes is calculated to be 0.74 from the peak areas of Fe and O, which is closely matched with the Fe/O value (0.78) estimated from the EDS analysis (Fig. 2b).

To understand the formation mechanism of the Fe_3O_4 nanoflakes, time-dependent experiments were conducted at 4, 8, 12 and 24 h, respectively. When the reaction was processed for 4 h, uniform nanoparticles with an average crystallite size of about 14.5 nm are obtained as the sole products (Fig. S3a and S4, ESI†). After a solvothermal treatment for 8 h, a small amount of flake-like congeries appear but nanoparticles are still the exclusive products (Fig. S3b, ESI†). With a longer reaction time (12 h), the product consists predominantly of Fe_3O_4 nanoflakes, however, nanoparticles with bigger diameters also exist in the product (Fig. S3c and d, ESI†). Finally, self-assembled Fe_3O_4 nanoflakes are obtained after 24 h (Fig. 1a). Based on the above results, the formation of Fe_3O_4 nanoflakes can be explained by a self-assembled process of metastable nanoparticles.

Generally, the intrinsic shape of nanocrystals is dominated by the crystalline structure of the initial seeds and the final shape is also governed by the subsequent growth stage *via* the delicate control of external factors.[15] It is known that an isotropic unit cell structure generally results in isotropic growth of particles and accordingly leads to a spherical morphology of the products.[16] Therefore, after the initial nucleation, owing to the cubic inverse spinel structure of Fe_3O_4 (Fig. S5, ESI†), the Fe_3O_4 monomers can grow into grain-like nanocrystals. Once the original Fe_3O_4 nanocrystals are formed in the hydrothermal system, to minimize the surface energies, they have a tendency to form aggregates by oriented assembly.[17] In the succedent self-assembled process, it was found that $[C_{16}mim]Cl$ plays a crucial role on the shape of the products. The isoelectric point of Fe_3O_4 is discovered to be pI = 6.4–6.8, and the surface of Fe_3O_4 is positively charged at pH $<$ 6.4 and negatively at pH $>$ 6.8.[18] The pH value is measured to be about 10.86 in the system, so the negative Fe_3O_4 surface may be caused by the adsorption of Cl^- on the Fe_3O_4. Along with the Cl^-, $[C_{16}mim]^+$ will also be aligned and arrayed along the primary Fe_3O_4 nanoparticles, driven by the Coulomb force with the Cl^-.[19] $[C_{16}mim]Cl$ has a strong tendency to self-aggregate into ordered structures which possess a large steric hindrance.[9,20] Therefore, they can provide special interlayer spaces for the oriented arrangement of Fe_3O_4 nanoparticles in the 2D direction. Hence, as the nanoscale building blocks coalesce, loose flake-like Fe_3O_4 aggregates are formed. Subsequently, the loose aggregates are crystallized *via* Ostwald ripening. Eventually, well-organized Fe_3O_4 nanoflakes are obtained. As above, the possible formation mechanism of the obtained Fe_3O_4 nanoflakes self-assembled from nanoparticles is illustrated in Fig. 3.

Controlled experiments with different IL contents from 0 to 0.1, 0.2 and 0.4 g were conducted to further substantiate the effect of $[C_{16}mim]Cl$ and the shape evolution of Fe_3O_4 is shown in Fig. S6, ESI.† Agglomerating nanoparticles can be obtained in the absence of $[C_{16}mim]Cl$. The products become gradually closer to pure nanoflakes in 0.4 g of $[C_{16}mim]Cl$. The results indicate that Fe_3O_4 nanoparticles can not be completly reacted with $[C_{16}mim]Cl$ if the content of the IL is relatively low as the particles tend to aggregate with each other, which can further prove the above deduction.

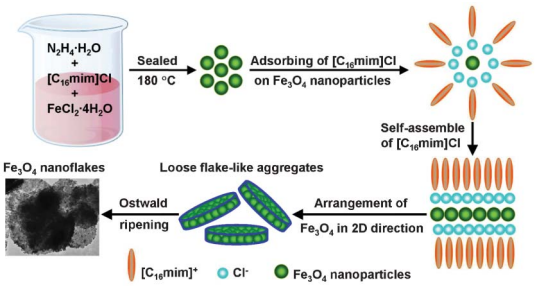

Fig. 3 Schematic illustration of the formation process of the Fe_3O_4 nanoflakes.

In addition, the properties of solvents can affect the solubility and diffusion behavior of the reactants.[21] Both literature[22] and experimental results indicate that glycerol has an influence on the formation of Fe_3O_4 nanoflakes. In the synthesis, a glycerol–water solvent was employed for two reasons: glycerol has a lower dielectric constant than water, which is beneficial for dissolving $[C_{16}mim]Cl$ to obtain uniform conditions and compared to the fast nucleation and aggregation in aqueous solutions, primary Fe_3O_4 nanoparticles are kinetically slower in glycerol–water due to the greater viscosity and fewer surface hydroxyls, which allows them to have enough time to find the low-energy configuration interface and undergo self-organization into the desired assemblies.[23] When glycerol is replaced by an equivalent volume of water and the other reaction parameters are unchanged, the products are composed of agglomerated Fe_3O_4 nanoparticles (Fig. S7, ESI†). We also tested the influence of the reaction temperature on this special superstructure and it was found that a temperature higher than 180 °C is favorable for the formation of nanoflakes (Fig. S8, ESI†).

The magnetic properties of the Fe_3O_4 nanoflakes were measured at 10 and 300 K and the results are shown in Fig. 4. The hysteresis loop of the nanoflakes shows a ferromagnetic-like property at 10 K. The saturation magnetization (M_s), coercivity (H_c) and remanent magnetization (M_r) are 69.66 emu g^{-1}, 547.5 Oe and 38.25 emu g^{-1}, respectively. It was reported that Fe_3O_4 nanocrystals can exhibit superparamagnetic behavior without a hysteresis loop as their size decreases to a certain value,[24] while for the as-synthesized Fe_3O_4 nanoflakes, there is a hysteresis loop and the H_c is 133.1 Oe at 300 K, indicating that the nanoflakes are multi-domain magnetite. Furthermore, the primary Fe_3O_4 nanoparticles do not fully grow together and many crystal defects or distortions exist in the gain boundaries (shown in Fig. 1a). In this regard, similar to nano-alloys,[25] a transition region with a domain-wall like structure may be formed in the grain boundaries (as indicated in Fig. 4) owing to the exchange-coupling interaction between the neighboring grains in the magnets.[26] Because of the domain-wall like structures, the coercivity of the obtained Fe_3O_4 nanoflakes is increased, which is beneficial for their potential application in high-density recording. In addition, at room temperature, the M_s of the Fe_3O_4 nanoflakes (64.52 emu g^{-1}) is comparatively lower than that of bulk magnetite (93 emu g^{-1}). This can be explained by the surface effect of small particles and a larger number of lattice defects.[27]

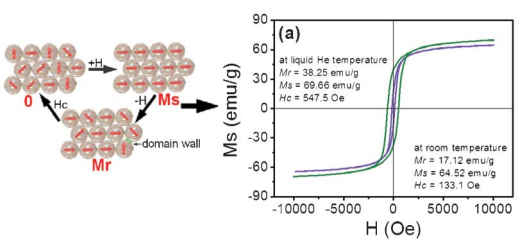

Fig. 4 Magnetization hysteresis curves recorded at 10 and 300 K of the Fe_3O_4 nanoflakes.

In conclusion, nanoparticle-assembled Fe_3O_4 nanoflakes with a uniform morphology and good dispersity have been synthesized. $[C_{16}mim]Cl$ plays an important part in controlling the shape of the Fe_3O_4 nanoflakes. The product has a special magnetic property, which may be beneficial for overcoming the "superparamagnetic limit" of Fe_3O_4 nanostructures. This synthetic method is expected to be extended to synthesize other metal oxides with intriguing structures.

This work is supported by the National Natural of Science Foundation of China (No. 20971070 and No. 20571044), 111 Project (B12015) and the Natural Science Foundation of Henan (No. 112300410224).

Notes and references

1 (*a*) V. Polshettiwar, B. Baruwati and R. S. Varma, *ACS Nano*, 2009, **3**, 728; (*b*) Q. Gao, A. Zhao, Z. Gan, W. Tao, D. Li, M. Zhang, H. Guo, D. Wang, H. Sun, R. Mao and E. Liu, *CrystEngComm*, 2012, **14**, 4834; (*c*) S. D. Tzeng, K. Lin, J. J. C. Hu, L. J. Chen and S. Gwo, *Adv. Mater.*, 2006, **18**, 1147; (*d*) C. Burda, X. Chen, R. Narayanan and M. A. El-Sayed, *Chem. Rev.*, 2005, **105**, 1025.

2 (*a*) J. Mu, B. Chen, Z. Guo, M. Zhang, Z. Zhang, P. Zhang, C. Shao and Y. Liu, *Nanoscale*, 2011, **3**, 5034; (*b*) G. Jian, Y. Liu, X. He, L. Chen and Y. Zhang, *Nanoscale*, 2012, **4**, 6336; (*c*) C. Yang, J. Wu and Y. Hou, *Chem. Commun.*, 2011, **47**, 5130; (*d*) M. Zhu and G. Diao, *J. Phys. Chem. C*, 2011, **115**, 18923.

3 (*a*) Z. Liu, D. Zhang, S. Han, C. Li, B. Lei, W. Lu, J. Fang and C. Zhou, *J. Am. Chem. Soc.*, 2005, **127**, 6; (*b*) Z. Huang, Y. Zhang and F. Tang, *Chem. Commun.*, 2005, 342.

4 (*a*) L. Han, Y. Chen and Y. Wei, *CrystEngComm*, 2012, **14**, 4692; (*b*) W. Dong, X. Li, L. Shang, Y. Zheng, G. Wang and C. Li, *Nanotechnology*, 2009, **20**, 035601; (*c*) X. Li, Z. Si, Y. Lei, X. Li, J. Tang, S. Song and H. Zhang, *CrystEngComm*, 2011, **13**, 642.

5 J. Gong, S. Li, D. Zhang, X. Zhang, C. Liu and Z. Tong, *Chem. Commun.*, 2010, **46**, 3514.

6 L. Zhang, J. Wu, H. Liao, Y. Hou and S. Gao, *Chem. Commun.*, 2009, 4378.

7 (*a*) R. E. Morris, *Angew. Chem., Int. Ed.*, 2008, **47**, 442; (*b*) J. S. Wilkes, *Green Chem.*, 2002, **4**, 73; (*c*) X. Liu, X. Duan, P. Peng and W. Zheng, *Nanoscale*, 2011, **3**, 5090; (*d*) W. Zheng, X. Liu, Z. Yan and L. Zhu, *ACS Nano*, 2009, **3**, 115; (*e*) X. Liu, J. Ma, P. Peng and W. Zheng, *Langmuir*, 2010, **26**, 9968; (*f*) X. Li, D. Liu, S. Song, X. Wang, X. Ge and H. Zhang, *CrystEngComm*, 2011, **13**, 6017; (*g*) J. Lian, J. Ma, X. Duan, T. Kim, H. Li and W. Zheng, *Chem. Commun.*, 2010, **46**, 2650.

8 X. Bai, L. Zheng, N. Li, B. Dong and H. Liu, *Cryst. Growth Des.*, 2008, **8**, 3840.
9 J. Ma, X. Liu, J. Lian, X. Duan and W. Zheng, *Cryst. Growth Des.*, 2010, **10**, 2522.
10 (*a*) J. F. Banfield, S. A. Welch, H. Zhang, T. T. Ebert and R. L. Penn, *Science*, 2000, **289**, 751; (*b*) T. D. Nguyen, D. Mrabet and T. O. Do, *J. Phys. Chem. C*, 2008, **112**, 15226.
11 L. S. Zhong, J. S. Hu, H. P. Liang, A. M. Cao, W. G. Song and L. J. Wan, *Adv. Mater.*, 2006, **18**, 2426.
12 Y. Tian, B. Yu, X. Li and K. Li, *J. Mater. Chem.*, 2011, **21**, 2476.
13 (*a*) J. Lu, X. Jiao, D. Chen and W. Li, *J. Phys. Chem. C*, 2009, **113**, 4012; (*b*) X. W. Teng, D. Black, N. J. Watkins, Y. L. Gao and H. Yang, *Nano Lett.*, 2003, **3**, 261.
14 A. P. Grosvenor, B. A. Kobe, M. C. Biesinger and N. S. McIntyre, *Surf. Interface Anal.*, 2004, **36**, 1564.
15 S. M. Lee, S. N. Cho and J. Cheon, *Adv. Mater.*, 2003, **15**, 441.
16 (*a*) W. Du, X. Qian, X. Ma, Q. Gong, H. Cao and J. Yin, *Chem.–Eur. J.*, 2007, **13**, 3241; (*b*) S. H. Sun and H. Zeng, *J. Am. Chem. Soc.*, 2002, **124**, 8204.
17 G. Xi, C. Wang and X. Wang, *Eur. J. Inorg. Chem.*, 2008, 425.
18 H. H. Lee, S. Yamaoka, N. Murayama and J. Shibata, *Mater. Lett.*, 2007, **61**, 3974.
19 Y. Zhou, J. H. Schattka and M. Antonietti, *Nano Lett.*, 2004, **4**, 477.
20 (*a*) A. Taubert, *Angew. Chem., Int. Ed.*, 2004, **43**, 5380; (*b*) Y. Zhou and M. Antonietti, *Adv. Mater.*, 2003, **15**, 1452.
21 F. Xue, H. Li, Y. Zhu, S. Xiong, X. Zhang, T. Wang, X. Liang and Y. Qian, *J. Solid State Chem.*, 2009, **182**, 1396.
22 (*a*) C. Wang, D. Chen and X. Jiao, *J. Phys. Chem. C*, 2009, **113**, 7714; (*b*) H. Li, Z. Bian, J. Zhu, D. Zhang, G. Li, Y. Huo, H. Li and Y. Lu, *J. Am. Chem. Soc.*, 2007, **129**, 8406; (*c*) B. Li, Y. Xie, Y. Xu, C. Wu and Z. Li, *J. Solid State Chem.*, 2006, **179**, 56.
23 (*a*) A. P. Alivisatos, *Science*, 2000, **289**, 736; (*b*) L. P. Zhu, H. M. Xiao, W. D. Zhang, G. S. Yang and Y. Fu, *Cryst. Growth Des.*, 2008, **8**, 957.
24 (*a*) Y. Liu, W. Jiang, S. Li and F. S. Li, *Appl. Surf. Sci.*, 2009, **255**, 7999; (*b*) L. Zhang, S. Z. Qiao, Y. G. Jin, Z. G. Chen, H. C. Gu and G. Q. Lu, *Adv. Mater.*, 2008, **20**, 805.
25 H. W. Zhang, T. Y. Zhao, C. B. Rong, S. Y. Zhang, B. S. Han and B. G. Shen, *J. Magn. Magn. Mater.*, 2003, **267**, 224.
26 (*a*) J. B. Lian, X. C. Duan, J. M. Ma, P. Peng, T. Kim and W. J. Zheng, *ACS Nano*, 2009, **3**, 3749; (*b*) L. P. Zhu, H. M. Xiao and S. Y. Fu, *Cryst. Growth Des.*, 2007, **7**, 177.
27 (*a*) X. Liang, X. Wang, J. Zhuang, Y. Chen, D. Wang and Y. Li, *Adv. Funct. Mater.*, 2006, **16**, 1805; (*b*) N. A. D. Burke, H. D. H. Stover and F. P. Dawson, *Chem. Mater.*, 2002, **14**, 4752.